International Journal of Advanced Trends in Engineering and Management
(ISSN 2583-7052)

Vol. IV, No. 06, pp. 1-11, June

Advancing Bone Fracture Risk Assessment and prediction through Spiking Neural Network

S. Komalavalli[1], A. Amutha[2]

[1]Assistant Professor, Department of Electronics and Communication Engineering, Einstein College of Engineering, Tirunelveli, 627012. komalavallimuralidharan@gmail.com

[2]Assistant Professor, Department of Electrical and Electronics Engineering, Dhanalakshmi Srinivasan College of engineering, Coimbatore, 641105, India. amuthaa@dsce.ac.in

***Corresponding Author E-mail**: **komalavallimuralidharan@gmail.com**

ABSTRACT: Bone Fracture (BF) is one of the most prevalent health issues affecting people, caused by accidents or medical conditions like bone cancer. This paper proposes a Spiking Neural Network (SNN), an innovative approach for detecting bone fractures. To identify fracture and non-fracture X- ray images, the input image is taken from bone fracture detection dataset that incorporates advanced techniques. Initially, image resizing and the Adaptive Gabor Filter (AGF) is applied to the dataset to resize the images and remove unwanted noise. Next, the processed images are segmented using Kernel K-means clustering, which helps locate clusters that are not linearly separable with bone fractures. The segmented images are then extracted by using Principal Component Analysis (PCA) addressing the over fitting problem and aiding in data reduction for further analysis. Finally, a SNN framework is proposed to enhance the prediction of bone fractures from X-ray images, overcoming challenges in risk analysis. The SNN classifies X-ray images as either fractured or non-fractured. The proposed approach is implemented using Python software and demonstrates that the SNN classifier achieves an improved accuracy of 96% compared to other techniques.

Keywords: Spiking Neural Network (SNN), Principal Component Analysis (PCA), Kernel K-means clustering, Adaptive Gabor Filter (AGF), Image Resizing, Bone Fracture (BF)

1. Introduction

According to certain theories, the human body has 206 bones and they differ in size, form, and complexity [1]. The ear canal contains the smallest bone, while the femur is the largest. Fractures in the lower leg bones are frequently observed [2]. Conversely, skeletal fracture occur at any time, early detection and treatment are crucial. Unfortunately, even in the wealthiest nations, bone fractures are becoming increasingly common in worldwide [3]. Medical images are distributed via the Digital Imaging and Communications in Medicine (DICOM) standard [4]. Among the various tools used to produce the biological image, X-rays are one of the most widely used for identifying bone fractures as they are quick, affordable, and user-friendly [5]. Notably, Wilhelm Roentgen discovered X-rays in 1895 for medical imaging, and they have since become a crucial component of modern diagnostics [6]. Moreover, digital X-ray imaging equipment is now widely utilized in many medical settings due to its portability and advancements in computerized image processing [7].

To remove unwanted noise and to attain high quality image, a pre-processing technique is applied. Using the pre-processing technique such as Gaussian filtering and Adaptive Histogram Equalization, the noises are eliminated and

contrasts of bone fracture x-ray image are improved. However, large kernel size are computationally expensive [8]. Conversely, to find the missing values in the bone fracture image Synthetic Minority Over-sampling Technique (SMOTE) is used. SMOTE is a valuable tool to handle unbalanced data with good performance. Although the model over fit to the enhanced data, SMOTE lessen over fitting to the original dataset [9]. To overcome this limitation, the proposed pre-processing technique used here is AGF which removes the unwanted noise and produce clear, and filtered image.

Whereas, using femur segmentation the bone fracture risk is identified and segmented. It is a more precise for diagnosis and analysis, as well as makes surgical plan easier. Difficulty in complex algorithms and the possibility of mistakes on overlapping structures and image noise [10]. Moreover, to segment the bone fracture Semantic segmentation is used. More effective and improve accuracy by eliminating background noise. However, it is difficult for some applications since it needs a lot of labelled data and computationally costly [11]. To overcome this limitation the proposed segmentation technique used here is Kernel K-means clustering which is to locate the cluster value and segment the bone fracture image.

To improve the extraction and characterization of bone fractures, Gray Level Co-Occurrence Matrix (GLCM) is used. It extracts different texture information, records spatial relationships between pixels, and increase classification accuracy. The matrixes have huge complexity, and possible feature correlations are the drawback of GLCM feature [12-13]. Whereas, Finite Beta Gaussian Mixture Model (FBGMM), identies bone fractures quickly and constantly by including data from X-rays. FBGMMs require more reliable parameter estimation methods due to their increased computational complexity [14]. To overcome this limitation, the proposed PCA based feature extraction technique used, which mitigates over fitting problem, data dimension, and reduction in bone fracture image.

Furthermore, a binary-class Convolutional Neural Network (CNN) model is used to identify bone fracture. Automatically identify patterns and learn characteristics, according to the input. It have the possibility of over fitting problem, necessity for large datasets [15]. To overcome the limitation of bone fracture risk SNN is used. It classifies the image with higher accuracy and performance.

2. Related work

Kandel *et al* [16] (2020) have proposed a CNN with VGG to classify musculoskeletal images on bone fractures. Its architecture covers number of layers produces extremely precise image classification. However, it is inefficient because it consumes a significant amount of time and storage space.

Ma and Luo [17] (2021) have proposed a Crack-Sensitive Convolutional Neural Network (CrackNet) and Faster region based CNN (Faster R-CNN) algorithm to classify the bone fracture with high accuracy and performance. Using CrackNet, finds the fracture lines, which are detected successfully and preciously. Moreover, Faster R-CNN produces less accurate localizations because it requires a fixed-size input.

Rashid *et al* [18] (2023) have proposed a CNN with Long Short Term Memory (CNN-LSTM) to detect wrist fractures from X-ray images. CNN-LSTM classifies with higher accuracy compared to other technique. However, CNN-LSTM models are computationally expensive, needing a substantial amount of memory and computing capacity.

Bagaria *et al* [19] (2021) have proposed a Support Vector Machine (SVM) and Error Back propagation Neural Network (EBP-NN) to detect the fractured and non-fractured bone images. The SVM methods are more effective and have a better classification rate. Moreover, they need

additional hyper parameter adjustment and take longer to train.

Fang *et al* [20] (2025) have proposed a Faster R-CNN with recognition model to detect the bone fracture. The Faster R-CNN with recognition model is reliable enough too accurately and efficiently identify and classify the region of fractured and non-fractured. However, slow convergence and local minima susceptibility are two drawbacks of Faster R-CNN with recognition model.

The contribution of this study is summarized as follows:

- The pre-processing technique such as image resizing and AGF reduces the noise present in the images and enhances the image resolution.
- For better segmentation, the bone X-ray image locates its cluster values using Kernel K-means clustering.
- PCA reduces the data reduction, dimension and mitigates the over fitting problem for bone X-ray image.
- SNN classifier is developed, to enhance bone fracture risk accuracy and efficiency.
- Validates the proposed model using metrics like accuracy, precision, recall, F1-score, and AUC, demonstrating significant improvement over existing methods.

3. Proposed work

The block diagram of the proposed work is depicted in figure 1 the SNN is to find the bone fracture in the X-ray images. Initially, the image is resized using the image resizing method and removes the unwanted noise using AGF. Next, the processed image is given to the segmentation step now the Kernel K-means clustering is used. Kernel K-means clustering method locates the cluster values for further analysis.

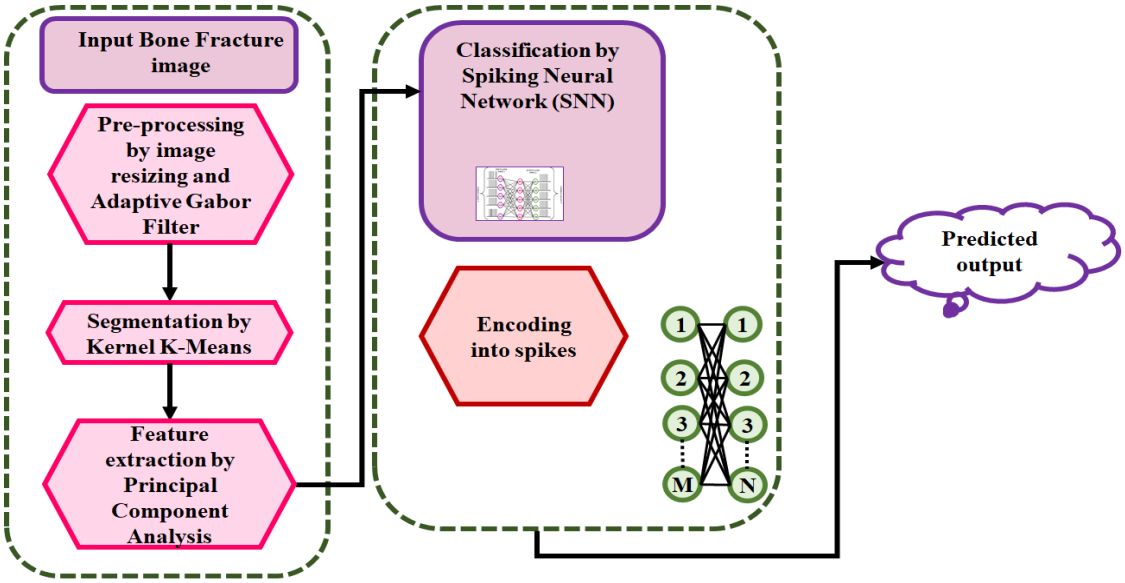

Figure 1: *Block diagram of proposed work*

Next, the segmented output is given as an input to PCA, for further analysis. PCA extracts the data compression and data reduction in dimensions. Finally, a proposed SNN is utilized to increase the accuracy and efficiency of the bone fractured and non-fractured X-ray images. SNN improve model accuracy, performance metrics for the bone fracture.

3.1 Pre-processing for Bone Fracture Risk

In the bone fracture identification, pre-processing approach comprises of two methods image resizing, and Adaptive Gabor Filter.

3.1.1 Image resizing

The purpose of the preprocessing stage is to enhance the bone fracture image by eliminating unwanted distortions and background noise. It improves the features of images for analysis and processing. The RGB-formatted images are resized to their standard sizes. The HSV format is then applied to these RGB images that have been resized. Resizing the image to a standard matrix improves computation accuracy and performance.

3.1.2 Adaptive Gabor Filter (AGF)

Data pre-processing is the initial stage here AGF method is used to filter the bone X-ray image. The best characteristics in bone fracture that enable multi-resolution analysis to extract the optimal bone fracture attributes in the frequency and spatial domains are AGF. Whereas, the sine component provides the directionality, the Gaussian component creates the weights. The 2D Gabor filter described in this paper it is represented by the following equations:

$$g = \exp\left(-\frac{x'^2+\acute{\gamma}^2y'^2}{2\sigma^2}\right)\exp(i\,(2\pi\frac{x'}{\lambda}+\psi)) \quad (1)$$

$$g_{re} = \exp\left(-\frac{x'^2+\acute{\gamma}^2y'^2}{2\sigma^2}\right)\cos(\,2\pi\frac{x'}{\lambda}+\psi) \quad (2)$$

Where,

$$x' = x\cos\theta + y\sin\theta\,, y' = -x\sin\theta + y\cos\theta \quad (3)$$

The real part g_{re} of the Gabor function is utilized for the practical implementation of bone fracture prediction. The wavelength of the sinusoidal function is represented by λ for the Gabor function, where $f = \frac{1}{\lambda}$ and f is the sinusoidal frequency. The Gabor-function support's ellipticity is specified by θ, denotes the normal orientation to parallel stripes ψ, indicates the phase offset, θ denotes the Gaussian envelope's standard deviation and γ represents the spatial aspect ratio. The value of ψ is often between 0 and π, the range of θ is between 0 and π, and γ typically takes the value of 1. Followed by pre-processing the input image is given to the segmentation process to segment the bone fracture image.

3.2 Segmentation by Kernel K-means clustering

The pre-processed bone X-ray image is given as an input to the Kernel K-means clustering. A simplification of kernel is the traditional k-means method used to segment the bone fracture. Kernel applies k-means in bone fracture after mapping data points from input to a higher dimensional feature using a non-linear transformation φ. This leads to feature space linear separators that match input space nonlinear separators. The kernel k-means technique uses the kernel trick to solve this issue by applying k-means on the induced feature space after translating data with non-linear transformation into the proper feature space. Whereas these clusters are not linearly separable in the original space, these results in linearly separated clusters in the new feature space in figure 2.

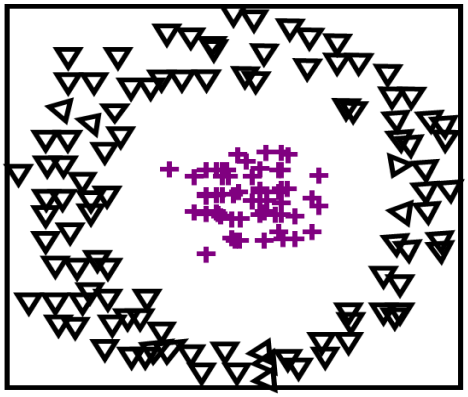

Figure 2: *Kernel K-means clustering*

In the new feature space, these clusters are linearly separated, even though they are not linearly separable in the original space. $\varphi : R^d \rightarrow H$ represent a kernel mapping between the original and kernel spaces. A kernel function $(x,z) = \varphi(x)T\,\varphi(z)$ induces H, a Reproducing Kernel Hilbert Space (RKHS). Then $\varphi(x) = [\varphi(x_1),\varphi(x_2),\cdots,\varphi(x_n)]$, and the kernel space's robust k-means in equation is as follows:

$$E(x_1, \ldots\ldots, x_n) = \sum_{i=1}^{n} \sqrt{\sum_{j=1}^{c} z_{ij} (\|\varphi(x_i) - v_j\|)^2} \quad (4)$$

Where, $v_j = \sum_{i=`1}^{N} a_{ij} \varphi(x_i)$

Where a_{ij} the membership of is x_i belongs to j^{th}cluster. Spectral approaches, which calculate the eigenvectors of the kernel matrix, are commonly used to address these problems. Spectral techniques are effective because they compute globally optimal solutions of a relaxation of the issue. Kernel k-means removes and calculate Eigen vectors. It determines the optimal choice based on cluster initialization.

Table 1: *Kernel k-means algorithm*

Require: Data matrix $X \in \mathbb{R}^{nxd}$; Amount of clusters K; kernel function $k(x_1,x_2)$
Ensure: Cluster class class (j) for each sample x_j.
function $K_{ERNEL-K-MEANS}(X, c)$
Randomly modify class (j) to be an integer in $1,2, \ldots\ldots, K$ for each x_j.
while not converged do
for i ←1 to K do
Set S_i={$j \in \{1,2, \ldots\ldots, n\}: class(j) = i$}
for j← 1 to n do
set class (j) = $argmin_k$
Return S_i for $i = 1, 2, \ldots\ldots, c$.
end task

The kernel K-means gives the well segmented output. Next, the feature extraction for bone fracture is done by Principle Component Analysis.

3.3 Feature Extraction by Principle Component Analysis

PCA based feature extraction technique is used to analyse the bone fracture images. The challenge of fitting a low-dimensional affine subspace to a collection of data points in a high-dimensional space is known as PCA. PCA is a member of the dimension reduction family and is very helpful for large and massive and strongly correlated data in figure 3.

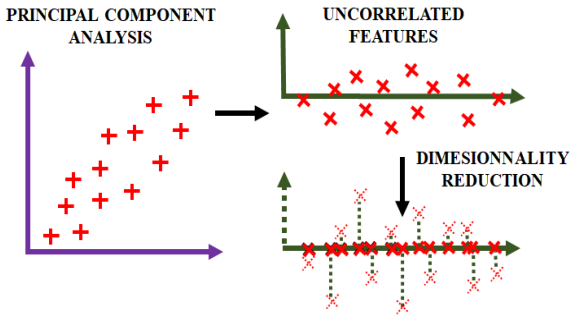

Figure 3: *PCA with dimensionality reduction*

PCA distribute with a smaller dataset rather than the original high-dimensional data. The PCA generates a collection of additional N variables $y_i$that are linear combinations of the first data set for a set of N $denotes$ arbitrary variables x_i(i $= 1, 2, \ldots, N$):

$$y_1 = a_{11}x_1 + a_{12}x_2 + \cdots + a_{1N}x_N \quad (5)$$

$$y_2 = a_{11}x_1 + a_{12}x_2 + \cdots + a_{1N}x_N \quad (6)$$

$$y_N = a_{N1}x_1 + a_{N2}x_2 + \cdots + a_{NN}x_N \quad (7)$$

It is feasible to minimize the dimensionality of those changed variables by taking the PCA that allow for the explanation of the maximum variances, where $K << N$. Since diagonalizing the original covariance matrix provides the explanation to this linear difficult, the percentage of variance explained by the first PCAs is determined by

$$\frac{\sum_{j=1}^{K} Var[y_j]}{Total\ variance} = \frac{\sum_{j=1}^{k} \lambda_j}{Trace(\sum_{NN})} = \frac{\sum_{j=1}^{k} \lambda_j}{\sum_{j=1}^{N} \lambda_j} \quad (8)$$

$$Trace(\sum_{NN}) = \sum_{i=1}^{N} \sigma_{ii}^2 = \sum_{i=1}^{N} \lambda_i \quad (9)$$

Where trace is the major diagonal of the covariance matrix as well as, $\sigma_{ii}^2 = Var[y_i], i = 1,2, \ldots\ldots, N$, λ_i stand eigenvalues, taken in descendent order. Following to this the extracted bone fracture image is given as input to the proposed SNN for bone fracture prediction.

3.4 Classification by Spiking Neural Network

The proposed SNN is utilized for effective classification of bone fracture. The general architecture moves from simple to sophisticated representations by progressively extracting and refining features from the incoming data.

Convolutional and pooling layers work together to improve the network's generalization and pattern recognition, which makes it useful for image recognition applications. More precisely, three consecutive convolutional layers, each measuring 3×3 and including $8, 64, 128$, and filters, respectively, are used in the suggested neural network architecture to process an i/p X-ray image. Specifically, a 4×4 max-pooling layer with a phase of is placed in among the second as well as third convolutional layers in figure 4.

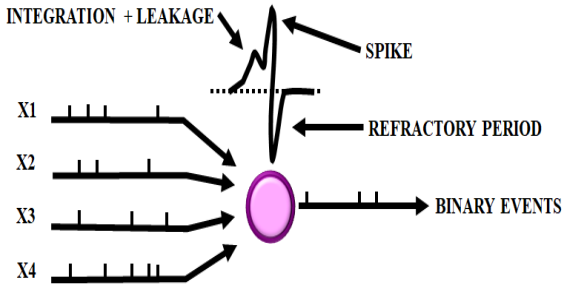

Figure 4: *Basic spiking neural network*

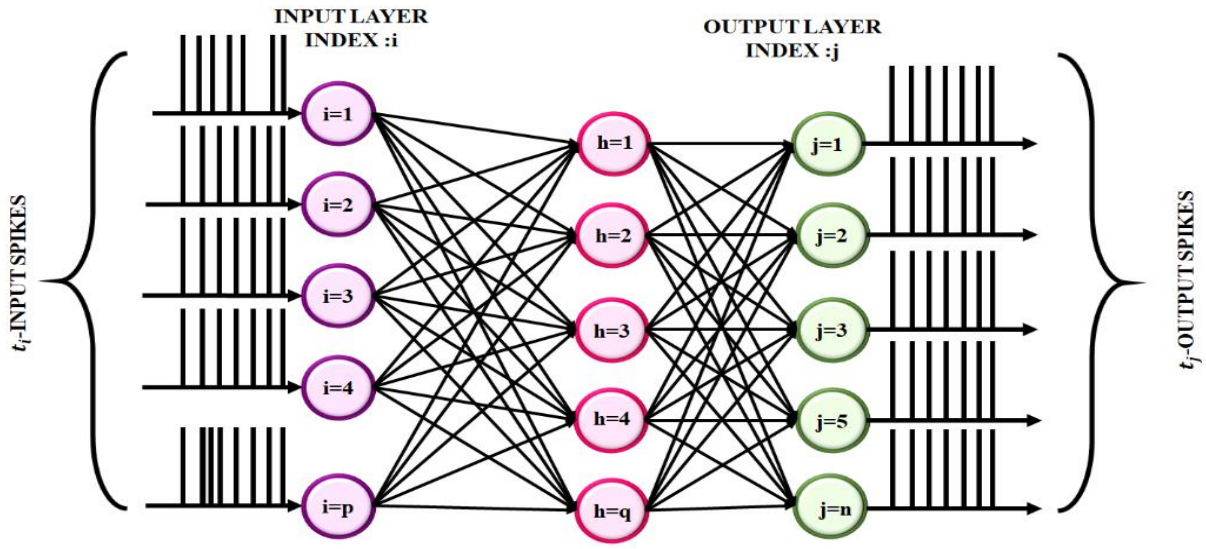

Figure 5: *SNN architecture*

In figure 5, the last fully connected layer, which is made up of dual neurons, uses the o/p from the third completely connected layer as its i/p. The output of a softmax function, a method for transforming neural network outputs into probabilities appropriate for classification problems, includes these neurons. This data is essential for the probabilities in order to enhance the classification task's overall performance. SNN produces good performances and better overall accuracy for the bone fracture X-ray images.

SNN have three such layers each with 128, 64, and 8 neurons are used. Except for the max-pooling layer, which does not require activation function these layers employ the spiking Rectified Linear Unit (ReLU) activation function. The ReLU activation function chosen primarily due to its great performance, computational economy, and ability to encourage sparsity in activations. Its straightforward formulation enables quick convergence during training and facilitates effective computations. Most significantly, the sparsity results in lower energy usage, which is vital for developing an energy-efficient SNN.

3.5 Result and Discussion

In this section the bone fractured and non-fractured X-ray images are predicted using the

proposed SNN. For identifying the fractured and non-fractured bone the dataset is taken from the kaggle.com. SNN is applied to train Bone fracture detection using X-ray images. Fractured and non-fractured bone is predicted using python software. The train images have the count of 700 and train images have the count of 700.

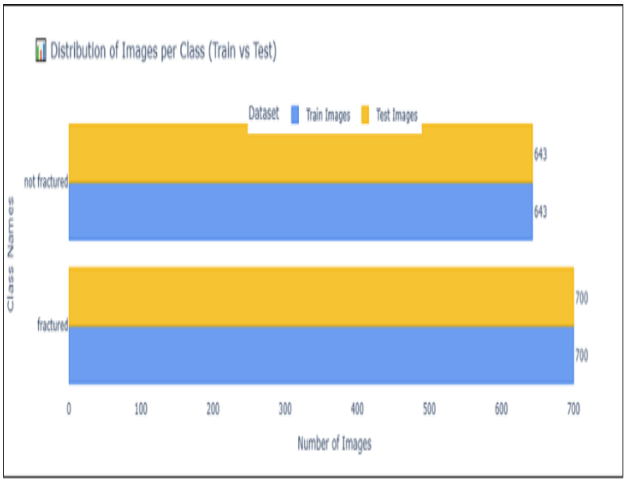

Figure 6: *Distribution of images per class*

Figure 6 shows the distribution of images per class for bone fracture image. Here the total number of fractured image for test is 700 and train is 700. Whereas, the total number of non-fractured image for test is 643 and train are 643. The bone fracture image is taken from the bone fracture X-ray dataset images.

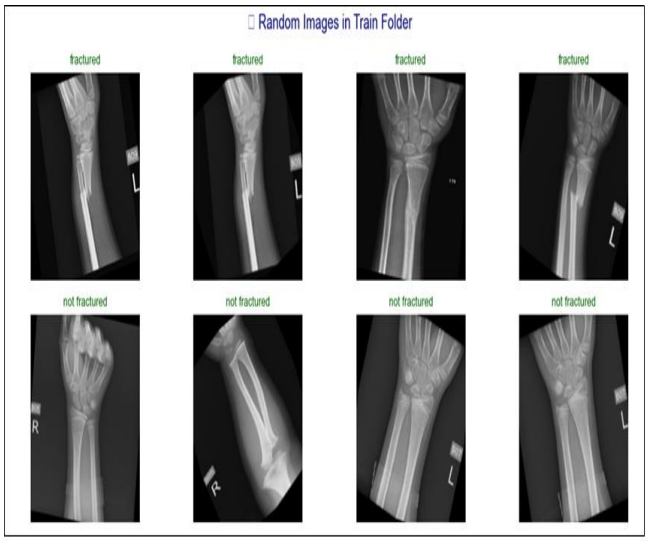

Figure 7: *Random image in training*

Figure 7 shows random images in train folder for fracture and non-fracture bone X-ray image. Here, the random images are taken from the bone fracture detection X-ray image dataset. Whereas, the eight image are randomly selected for fractured and non-fractured image.

Figure 8: *Input image*

Figure 8 shows the input bone X-ray image. Here the i/p image is taken from the bone fracture detection X-ray image dataset. Using the pre-processing techniques the input image is given to the image resizing technique.

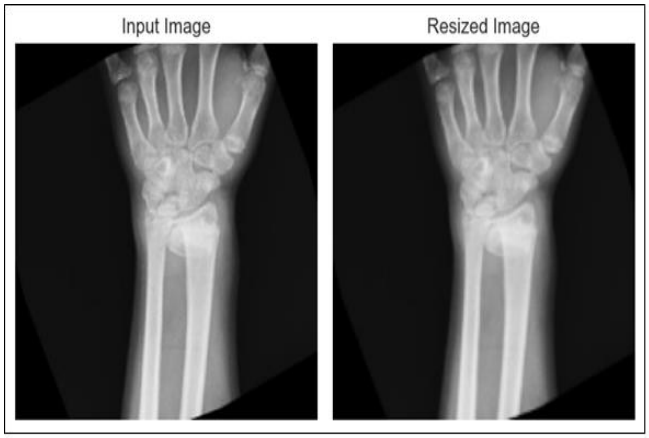

Figure 9: *Input image into resize image*

Figure 9 shows the input image into resized image bone X-ray image. The input bone image is resized for processing to get the good quality image. The images are resized by its pixel values. After that the resized image is given as an input to grayscale conversion technique for further processing.

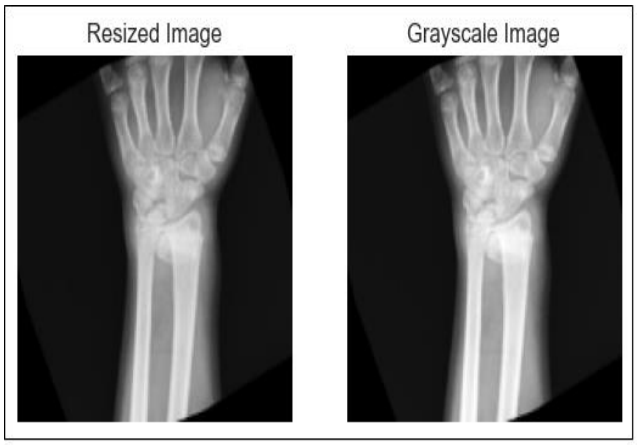

Figure 10: *Grayscale image*

Figure 10 shows the resize image into grayscale image for bone X-ray image. The resized image is converted into grayscale image using grayscale conversion technique. Here, the pixel values is converted into the single grayscale value. For each gray image there is a pixel value according to its gray value.

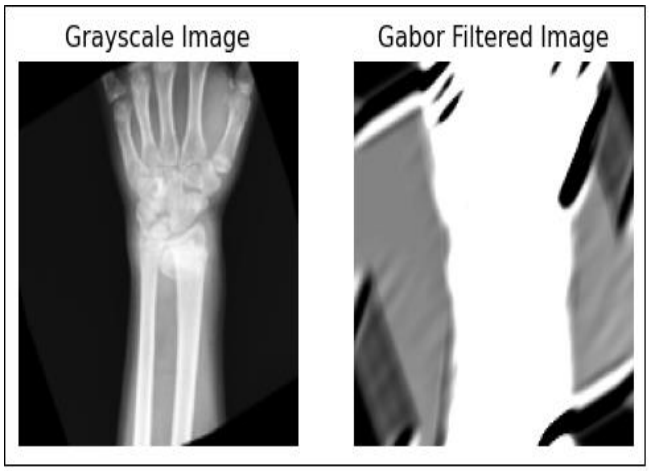

Figure 11: *Adaptive Gabor filter image*

Figure 11 shows the Grayscale image into adaptive Gabor filter for bone X-ray image. The grayscale bone X-ray image is given as an input to adaptive Gabor filter method. AGF method removes the noise in bone X-ray image for better quality image. Then the better quality AGF image is given as an input to segmentation technique.

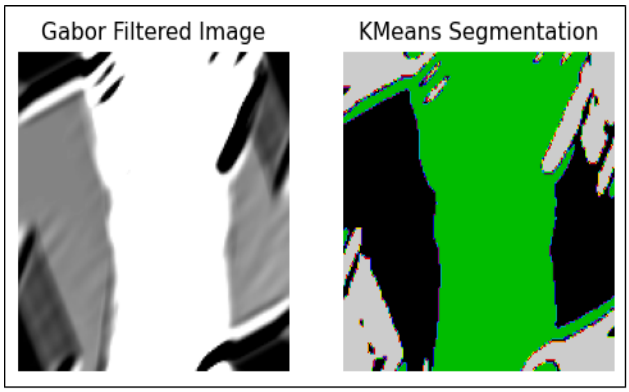

Figure 12: *Gabor filtered image into Kernel K-means*

Figure 12 shows the Gabor filtered image into Kernel K-means clustering for bone X-ray image. Locate the cluster values in bone X-ray image using Kernel k-Means clustering method. Bone region is separated with green color to segment the cluster value. The green color segmented image is given as a input to feature extraction approach.

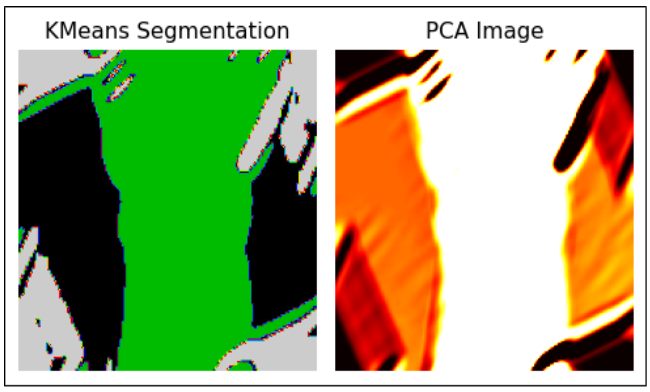

Figure 13: *Kernel-Kmeans into PCA*

Figure 13 shows the PCA for bone X-ray image. Here PCA captures the over fitting problems in the bone and shows the clear structure of bone X-ray image. It compresses and reduces the data reduction using PCA. PCA captures its over fitting problem and given as a input to classification.

4. Performance metrics

Performance criteria like accuracy, sensitivity and specificity which indicate the likelihood that a patient's bone will be correctly detected and appropriately diagnosed as the probabilities calculated by the SNN. The true positive, true

negative, false positive, and false negative results are denoted by TP, TN, FP, and FN, respectively. Sensitivity$[TP/(TP + FN)]$, specificity $[TN/(TN + FP)]$, F- value $[2 \times (recall \times precision)/(recall + precision)]$, and accuracy $[(TP + TN)/(TP + FP + FN + TN)]$.

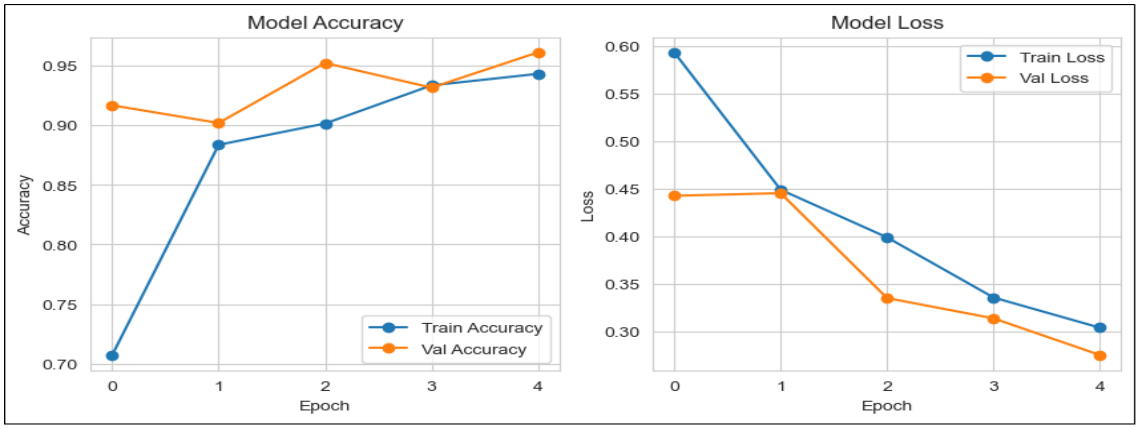

Figure 14: *Model accuracy and model loss*

Figure 14 shows the model loss and model accuracy. Model loss is reliable decline in training and validation loss, representing improved learning and reduced error. The X-axis denotes the epochs and Y-axis is accuracy for model accuracy simultaneously for model loss X-axis for epochs and Y-axis for loss. The Model Accuracy graph illustrates increasing accuracy of 96%, with the model achieving high performance and minimal over fitting.

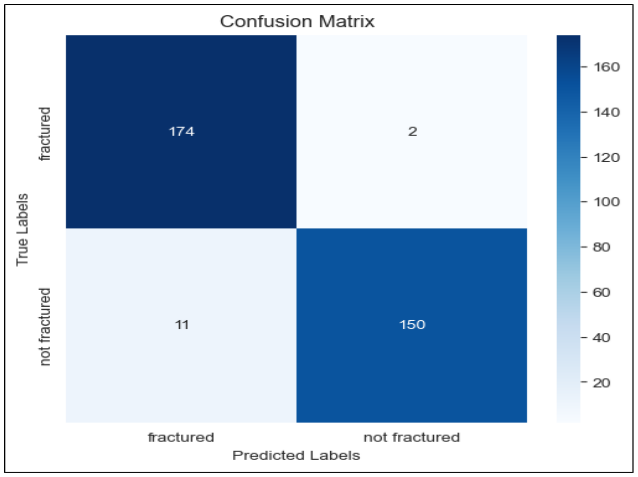

Figure 15: *Confusion matrix for proposed Spiking Neural Network*

Figure 15 shows the confusion matrix for proposed Spiking Neural Network. For this investigation, the following definitions are given: False Negative (FN), False Positive (FP), True Positive (TP), and True Negative (TN) are calculated for fractured and non-fractured bone X-ray image. Here the fractured image is 174 and non-fractured image is 150.

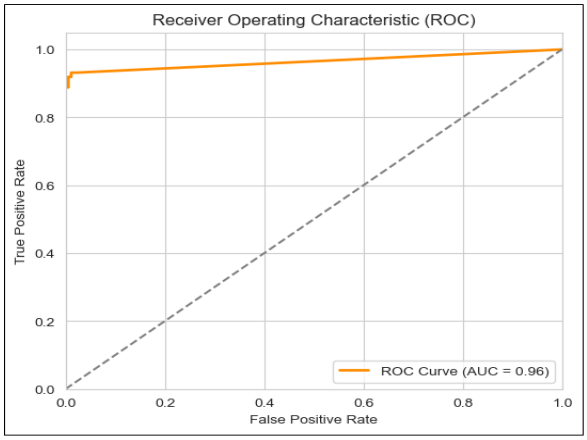

Figure 16: *ROC curve*

Figure 16 shows the ROC curve for fractured and non-fractured bone X-ray image. Here the ROC value for proposed SNN is 0.96. The ROC curve for the fractured and non-fractured bone X-ray image is calculated using the true positive rate and false positive rate.

5. Comparison for the proposed method

The comparison of proposed method with existing method is presented in table 2. The CrackNet and Faster R-CNN have the classification accuracy of 88.39% [17] and SVM-EBP-NN have the accuracy of 94% [18]. The

proposed SNN have the higher accuracy of 96% compared to the existing method in table 2. The proposed SNN have better performance.

Table 2: *Comparison for the proposed method*

Study	Method	Accuracy
Ma and Luo [17]	CrackNet and Faster R-CNN	88.39%
Rashid *et al.*[18]	SVM-EBP-NN	94%
Proposed approach	SNN	96%

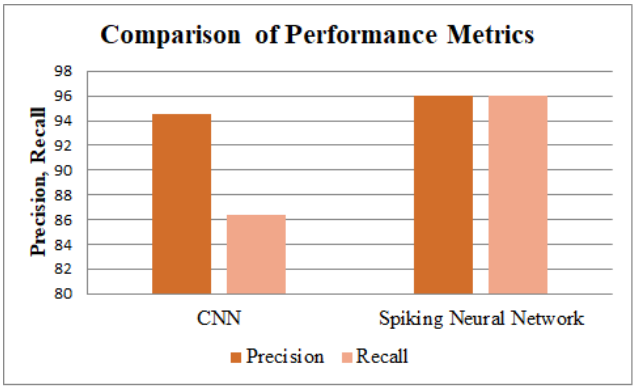

Figure 17: *Comparison for performance metrics*

Figure 17 shows the comparison for Precision and recall value. The CNN have the value of 94.51% and 86.39% [11] and proposed SNN have the precision value of 96% and recall of 96% for bone X-ray image.

6. Conclusion

In this study, SNN is proposed for the classification of bone fracture X-ray image. The preprocessing stage effectively enhances image quality by resized image and removed noised through AGF. The segmentation process is refined using Kernel K-means clustering which enhanced the located cluster values. Furthermore, PCA-based feature extraction captures the over fitting problems of bone fracture X-ray images. The performance evaluation, conducted on the Bone fracture detection X-ray dataset, demonstrates the superior capabilities of the SNN related to existing methods. The greater accuracy of 96% for SNN is achieved in contrast to the existing techniques.

References

1. F. Genest; L. Claußen; D. Rak; L. Seefried, Year: 2021, “Bone mineral density and fracture risk in adult patients with hypophosphatasia”, Osteoporosis International, Vol: 32, pp. 377-385.

2. Filippo Migliorini; Riccardo Giorgino; Frank Hildebrand; Filippo Spiezia; Giuseppe Maria Peretti; Mario Alessandri-Bonetti; Jörg Eschweiler; Nicola Maffulli, Year: 2021, “Fragility fractures: risk factors and management in the elderly”, Medicina, Vol: 57, No: 10, pp. 1119.

3. Daniel Dapaah; Daniel R. Martel; Faezeh Iranmanesh; Corin Seelemann; Andrew C. Laing; Thomas Willett, Year: 2023, “Fracture toughness: bridging the gap between hip fracture and fracture risk assessment”, Current Osteoporosis Reports, Vol: 21, No: 3, pp. 253-265.

4. Fei Yan; Linfeng Wu; Juan Lang; Zongju Huang, Year: 2024, “Bone density and fracture risk factors in ankylosing spondylitis: a meta-analysis”, Osteoporosis International, Vol: 35, No: 1, pp. 25-40.

5. Huimin Ma; Xintian Cai; Junli Hu; Shuaiwei Song; Qing Zhu; Yingying Zhang; Rui Ma, Year: 2024, “Association of systemic inflammatory response index with bone mineral density, osteoporosis, and future fracture risk in elderly hypertensive patients”, Postgraduate Medicine, Vol: 136, No: 4, pp. 406-416.

6. Beverley Catharine Craven; Christopher M. Cirnigliaro; Laura D. Carbone; Philemon Tsang; Leslie R. Morse, Year: 2023, “The pathophysiology, identification and management of fracture risk, sublesional osteoporosis and fracture among adults with spinal cord injury”, Journal of Personalized Medicine, Vol: 13, No: 6, pp. 966.

7. Shuaiwei Song; Xintian Cai; Junli Hu; Qing Zhu; Di Shen; Huimin Ma; Yingying Zhang, Year: 2024, “Effectiveness of spironolactone in reducing osteoporosis and future fracture risk in middle-aged

and elderly hypertensive patients", Drug Design, Development and Therapy, pp. 2215-2225.

8. Kosrat Dlshad Ahmed; Roojwan Hawezi, Year: 2023, "Detection of bone fracture based on machine learning techniques", Measurement: Sensors, Vol: 27, pp. 100723.

9. Ruhul Amin; Md Shamim Reza; Md Maniruzzaman; Md Al Mehedi Hasan; Hyoun-Sup Lee; Si-Woong Jang; Jungpil Shin, Year: 2023, "Intensive statistical exploration to identify osteoporosis predisposing factors and optimizing recognition performance with integrated GP kernels", IEEE Access, Vol: 11, pp. 131338-131350.

10. Pall Asgeir Bjornsson; Alexander Baker; Ingmar Fleps; Yves Pauchard; Halldor Palsson; Stephen J. Ferguson; Sigurdur Sigurdsson; Vilmundur Gudnason; Benedikt Helgason; Lotta Maria Ellingsen, Year: 2023, "Fast and robust femur segmentation from computed tomography images for patient-specific hip fracture risk screening", Computer Methods in Biomechanics and Biomedical Engineering: Imaging & Visualization, Vol: 11, No: 2, pp. 253-265.

11. Bo Chen; Hua Zhang; Guijin Wang; Jianwen Huo; Yonglong Li; Linjing Li, Year: 2023, "Automatic concrete infrastructure crack semantic segmentation using deep learning", Automation in Construction, Vol: 152, pp. 104950.

12. Gautam Amiya; Pallikonda Rajasekaran Murugan; Kottaimalai Ramaraj; Vishnuvarthanan Govindaraj; Muneeswaran Vasudevan; M. Thirumurugan; Yu-Dong Zhang; S. Sheik Abdullah; Arunprasath Thiyagarajan, Year: 2024, "Expeditious detection and segmentation of bone mass variation in DEXA images using the hybrid GLCM-AlexNet approach", Soft Computing, Vol: 28, No: 19; pp. 11633-11646.

13. Zhangtianyi Chen; Haotian Zheng; Junwei Duan; Xiangjie Wang, Year: 2023, "GLCM-Based FBLS: A Novel Broad Learning System for Knee Osteopenia and Osteoprosis Screening in Athletes", Applied Sciences, Vol: 13, No: 20, pp. 11150.

14. Santoshachandra Rao Karanam; Y. Srinivas; S. Chakravarty, Year: 2023, "A statistical model approach based on the Gaussian Mixture Model for the diagnosis and classification of bone fractures", International Journal of Healthcare Management, pp. 1-12.

15. K. C. Laxman; Nishat Tabassum; Li Ai; Casey Cole; Paul Ziehl, Year: 2023, "Automated crack detection and crack depth prediction for reinforced concrete structures using deep learning", Construction and Building Materials, Vol: 370, pp. 130709.

16. Ibrahem Kandel; Mauro Castelli; Aleš Popovič, Year: 2020, "Musculoskeletal images classification for detection of fractures using transfer learning", Journal of imaging, Vol: 6, No: 11, pp. 127.

17. Yangling Ma; Yixin Luo, Year: 2021, "Bone fracture detection through the two-stage system of crack-sensitive convolutional neural network", Informatics in Medicine Unlocked, Vol: 22, pp. 100452.

18. Tooba Rashid; Muhammad Sultan Zia; Talha Meraj; Hafiz Tayyab Rauf; Seifedine Kadry, Year: 2023, "A minority class balanced approach using the DCNN-LSTM method to detect human wrist fracture", Life, Vol: 13, No: 1, pp. 133.

19. Rinisha Bagaria; Sulochana Wadhwani; Arun Kumar Wadhwani, Year: 2021, "Bone fractures detection using support vector machine and error backpropagation neural network", Optik, Vol: 247, pp. 168021.

20. Qiong Fang; Anhong Jiang; Meimei Liu; Sen Zhao, Year: 2025, "Faster R-CNN model for target recognition and diagnosis of scapular fractures", Journal of Bone Oncology, Vol: 51, pp. 100664.